Northumbria Research Link

Northumbria University
NEWCASTLE

UniversityLibrary

Detection Performance to Spatially Random UAV Using the Ground Vehicle

Kezhi Wang, *Senior Member, IEEE*, Hongjiang Lei, *Senior Member, IEEE*, Gaofeng Pan, *Senior Member, IEEE*, Cunhua Pan, *Member, IEEE*, Yue Cao

.

Abstract—It is very challenging to detect an unmanned-aerial-vehicle (UAV) when it is applied to launch an attack by the enemy's country, due to its feature of mobility and flexibility. Against this background, in this paper, from wireless communication point of view, we study the detection probability of home country's ground vehicle (GV) to enemy's ground-station (GS)-to-UAV transmission system. We assume that the location of the GV is randomly distributed inside the space confined by the largest detection distance. Moreover, we assume the enemy's UAV is randomly distributed in the coverage space of the GS-to-UAV (G2A) transmission link but also keep the security distance from the GS. To this end, we first characterize the statistical features of the signal-to-noise-ratio (SNR) over the G2V and G2A links. Then, we define detection outage probability (DOP) and average detection capacity (ADC), and show their approximations. Finally, Monte-Carlo simulations are conducted to verify the correctness of our proposed analytical models.

Index Terms—Average Detection Capacity, Detection Outage Probability, Spatially Random UAV, Ground Vehicle.

I. INTRODUCTION

Recently, there is an growing popularity of applying unmanned aerial vehicles (UAVs) in a wide range of civilian applications, such as terrestrial communications, vehicular networks and entertainment areas [1], [2]. Additionally, the application of UAVs in military areas, such as surveillance and strikes have also been investigated in past years by several countries [3]. For instance, how to apply the UAV to launch attacks or conduct reconnaissance has been studied in [4].

On the other hand, it may be even more important to investigate how to prevent the home country from the attacks

K. Wang is with Department of Computer and Information Sciences, Northumbria University, NE1 8ST, UK (email: kezhi.wang@northumbria.ac.uk).

H. Lei is with the Chongqing Key Laboratory of Mobile Communications Technology, Chongqing University of Posts and Telecommunications, Chongqing 400065, China, and also with the Shaanxi Key Laboratory of Information Communication Network and Security, Xi'an University of Posts and Telecommunications, Xi'an 710121, China (e-mail: leihj@cqupt.edu.cn).

G. Pan is with School of Cyberspace Science and Technology, Beijing Institute of Technology, China (email: gaofeng.pan.cn@ieee.org)

C. Pan is with School of Electronic Engineering and Computer Science, Queen Mary University of London, London, E1 4NS, U.K. (email: c.pan@qmul.ac.uk)

Y. Cao is with Research Institute of Beihang University in Shenzhen, China. (email: 871441562@qq.com)

Corresponding Author: Hongjiang Lei

or reconnaissance from the UAVs deployed by the enemy country, from the national defence perspective. For instance, if the home country suffers the attack from enemy's UAV in emergency situations, it is essential to detect this UAV fast and effectively. However, this problem is rarely studied in the literature and is very challenging to solve. This is due to the fact that the enemy's UAV can move flexibly and freely in the 3-dimensional (3D) space and thus difficult to be detected. Furthermore, as the enemy's UAV always keeps changing its direction and position, which may further increase the difficulty of detection from the home country.

Motivated by the above observations, in this paper, we aim to investigate the detection probability of home country's ground vehicle (GV) to enemy's UAV system. To this end, we assume there is one hidden GS, deployed by the enemy to home country, trying to control its UAV via wireless link. Also, we assume the home country deploys a GV to detect the enemy's GS-to-UAV (G2A) communication link. We consider the randomness of the locations of the UAV and GV, by using the stochastic geometry theory. For G2A link, we assume that it is dominated by the large-scale fading, while for GS-to-GV (G2V) detection link, we assume it is not only affected by the large-scale fading but also by the small-scale fading, i.e., Nakagami fading.

Our proposed model can be applied to the emergency situation where the enemy invades the home country via UAV systems. Moreover, one can see that if the home country can successfully detect the enemy's UAVs via wireless communication channel, it may not only stop the attack or surveillance of the enemy's UAV, but also be able to possibly "hijack" or take over enemy's UAV to its own use. This is because if we can detect the communication signal of the enemy's UAV, we may decode/eavesdrop/crack their signal with further effort if possible and then send new control data to take over this UAV. The model may also be extended to enhance our physical layer security with some modifications, similar to [5]. This is due to fact that if we can detect the communication link of the enemy's UAV, we may possibly enhance our transmitted signal over their eavesdropping signals to guarantee our secure information transmission. Additionally, our analysis can be seen as the benchmark or upper bound of the scenarios where there are jammers deployed along with the enemy's UAV. The main contributions of the paper are summarized as follows:

- We define the detection outage probability (DOP) to capture the detection capacity of the GV from the home country to the enemy's UAV. The probability density function (PDF) and

cumulative distribution function (CDF) of the signal-to-noise-ratio (SNR) of both G2V and G2A links are characterized. To gain more insights, we obtain the lower bound of DOP in closed form.

• Furthermore, we present the average detection capacity (ADC) and to facilitate the analysis, we present the approximation of ADC, with the help of Meijer's G-function and Gaussian-Chebyshev quadrature.

II. SYSTEM MODEL AND STATISTICAL FEATURES

Consider a scenario that an enemy's UAV aims to attack or reconnoitre the home country. One hidden GS (G) is deployed by the enemy to the home country trying to communicate/guide this UAV (A) via G2A wireless system, as shown in Fig. 1. We also consider there is a GV (V) from
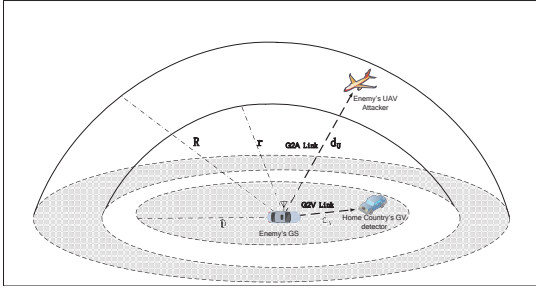

Fig. 1. Detection scenario of GV to the enemy's GS-to-UAV wireless system.

the home country, trying to detect the information transmitted from the enemy's GS to the UAV, via G2V links. Without loss of generality, we assume that the hidden GS is located in the center of a circle, where the GV is modelled as the randomly and uniformly distributed point, inside this circle. Define the radius of the circle as D ($D > 0$), which capture the largest detection distance of the G2V link. Also, define two hemispheres which share the common center where GS is located. The small hemisphere represents the area that the UAV will not fly into. This is realistic because if UAV flies close to the GS, it may be easily discovered. We also define a large hemisphere which decides the communication coverage of the G2A link. We model the UAV as the random point as well, uniformly distributed in the space inside the large hemisphere but outside the small hemisphere. Define the radius of the small hemisphere and large hemisphere as R ($R > 0$) and r ($r > 0$) respectively, with $R > r$.

Moreover, we define the transmit power at GS as P and the noise power of G2A and G2V as σ_a^2 and σ_v^2, respectively. For simplicity, we assume that $\sigma_a^2 = \sigma_v^2 = \sigma^2$, with the expectation value of $E\{\sigma^2\} = 1$. For the G2A link, we assume that it is dominated by the line-of-sight (LoS) channels. Therefore, the received SNR at the UAV can be given by $\gamma_U = \frac{\rho_U}{d_U^{\alpha_U}}$, where d_U denotes the distance between the ground station and UAV, $\rho_U = \frac{P\tau_U}{\sigma^2}$, α_U is the path loss exponent and τ_U captures the received channel gain, including carrier frequency, antenna gain, etc. Then, the CDF of d_U can be obtained as

$$F_{d_U}(x) = \begin{cases} 0, & x < r \\ \frac{x^3 - r^3}{R_0}, & r \le x \le R \\ 1, & x > R \end{cases} \quad (1)$$

where $R_0 = R^3 - r^3$.

Lemma 1. The CDF and PDF of γ_U can respectively be

$$F_{\gamma_U}(x) = \begin{cases} 0 & x < \frac{\rho_U}{R^{\alpha_U}} \\ 1 - \frac{(\rho_U)^{\frac{3}{\alpha_U}} x^{-\frac{3}{\alpha_U}} - r^3}{R_0} & \frac{\rho_U}{R^{\alpha_U}} \le x \le \frac{\rho_U}{r^{\alpha_U}} \\ 1 & x > \frac{\rho_U}{r^{\alpha_U}} \end{cases}, \quad (2)$$

$$f_{\gamma_U}(x) = \begin{cases} \frac{3(\rho_U)^{\frac{3}{\alpha_U}} x^{-\frac{3}{\alpha_U}-1}}{\alpha_U R_0} & \frac{\rho_U}{R^{\alpha_U}} \le x \le \frac{\rho_U}{r^{\alpha_U}} \\ 0 & \text{otherwise} \end{cases}. \quad (3)$$

Proof: Similar to [6], [7], [8], the CDF of γ_U is as

$$F_{\gamma_U}(x) = \Pr\{\gamma_U \le x\} = 1 - \Pr\left\{d_U \le \left(\frac{\rho_U}{x}\right)^{\frac{1}{\alpha_U}}\right\}$$
$$= 1 - F_{d_U}\left(\left(\frac{\rho_U}{x}\right)^{\frac{1}{\alpha_U}}\right). \quad (4)$$

By using (1), one obtains the CDF of γ_U as (2). By taking the first-order derivative of (2), one obtains the PDF as (3). ∎

For the G2V link, we consider it is affected by both large-scale signal loss and small-scale fading. Thus, the received SNR at GV is modeled as $\gamma_V = \frac{\rho_V |g_{SV}|^2}{(d_V)^{\alpha_V}}$, where $\rho_V = \frac{P\tau_V}{\sigma^2}$, τ_V is the received channel gain at GV, including carrier frequency, antenna gain, etc, d_V denotes the distance between the GV and GS, α_V is the path loss exponent, g_{SV} denotes the small-scale fading following the Nakagami-m distribution with CDF given by [9] $F_{|g_{SV}|^2}(x) = 1 - e^{-\frac{m}{\Omega}x} \sum_{i=0}^{m-1} \left(\frac{m}{\Omega}\right)^i \frac{x^i}{i!}$, where m is shape parameter, which is assumed to be integer number, and Ω represents the average channel power gains.

Then, one has the CDF of distance d_V as

$$F_{d_V}(x) = \begin{cases} 0, & x < 0 \\ \frac{x^2}{D^2}, & 0 \le x \le D \\ 1, & x > D \end{cases}. \quad (5)$$

Next, we apply the following lemma to show the statistical features of γ_V.

Lemma 2. One can have the CDF of γ_V given as follows in terms of Meijer's G-function:

$$F_{\gamma_V}(x) = 1 - \frac{2(\eta_1 x)^{-\frac{2}{\alpha}}}{D^2\alpha} \sum_{i=0}^{m-1} \frac{1}{i!} \Upsilon\left(i + \frac{2}{\alpha}, \eta_1 D^\alpha x\right)$$
$$= 1 - \frac{2}{\alpha_V} \sum_{i=0}^{m-1} \frac{1}{i!} G_{1,2}^{1,1}\left[\eta_2 x \begin{vmatrix} 1-\frac{2}{\alpha_V} \\ i, -\frac{2}{\alpha_V} \end{vmatrix}\right], \quad (6)$$

where $\eta_1 = \frac{m}{\Omega\rho_V}$, $\eta_2 = \frac{mD^{\alpha_V}}{\Omega\rho_V}$, $\Upsilon(\cdot, \cdot)$ is the lower incomplete Gamma function, as defined in [10, (8.350.1)], and $G_{p,q}^{m,n}[\cdot]$ is the Meijer's G-function as defined in [10, (9.301)].

Proof: By utilizing [10, (8.351.1)], [10, (9.31.5)] and [11,

8.4.16.1], the CDF of γ_V is given by

$$
\begin{aligned}
F_{\gamma_V}(x) &= \Pr\{\gamma_V \le x\} = \Pr\left\{\frac{\rho_V|g_{SV}|^2}{(d_V)^{\alpha_V}} < x\right\} \\
&= \Pr\left\{|g_{SV}|^2 < \frac{(d_V)^{\alpha_V}}{\rho_V}x\right\} = \int_0^\infty F_{|g_{SV}|^2}\left(\frac{t^{\alpha_V}}{\rho_V}\right) f_{d_V}(t)\,dt \\
&= 1 - \frac{2}{D^2}\sum_{i=0}^{m-1}\frac{(\eta_1 x)^i}{i!}\int_0^D t^{i\alpha_V+1}\exp(-\eta_1 t^{\alpha_V})\,dt \\
&= 1 - \frac{2(\eta_1 x)^{-\frac{2}{\alpha}}}{D^2\alpha}\sum_{i=0}^{m-1}\frac{1}{i!}\Upsilon\left(i+\frac{2}{\alpha},\eta_1 D^\alpha x\right) \\
&= 1 - \frac{2}{\alpha_V}\sum_{i=0}^{m-1}\frac{1}{i!}G_{1,2}^{1,1}\left[\eta_2 x\,\Big|\,{1-\frac{2}{\alpha_V} \atop i,-\frac{2}{\alpha_V}}\right],
\end{aligned}
\tag{7}
$$

where $\eta_1 = \frac{m}{\Omega\rho_V}$, $\eta_2 = \frac{mD^{\alpha_V}}{\Omega\rho_V}$, $\Upsilon(\cdot,\cdot)$ is lower incomplete Gamma function defined by [10, (8.350.1)], and $G_{p,q}^{m,n}[\cdot]$ is Meijer's G-function, defined by [10, (9.301)] and [12]. ∎

III. DETECTION OUTAGE PROBABILITY

The detection probability is defined as that the instantaneous channel capacity of G2V is higher than that of G2A. In this case, it is possible for the GV from home country to detect and/or eavesdrop the wireless communication between the enemy's ground station and its UAV, similarly to the idea of physical layer security. As a result, the home country may defend itself against the attack from the enemy's UAV. To this end, the instantaneous detection capacity is expressed as

$$
C_s(\gamma_V,\gamma_U) = \max\{\log_2(1+\gamma_V) - \log_2(1+\gamma_U), 0\}.
\tag{8}
$$

In (8), the detection event is encountered when the instantaneous detection capacity of G2V to G2A link becomes higher than the detection rate threshold, C_{th} $(C_{th} \ge 0)$. Then, one can write the DOP as

$$
\begin{aligned}
P_{\text{DOP}} &= \Pr\{C_s \le 2^{C_{th}}\} = \Pr\left\{\frac{1+\gamma_V}{1+\gamma_U} \le \Theta\right\} \\
&= \Pr\{\gamma_V \le \Theta\gamma_U + \Theta - 1\} \\
&= \int_0^\infty F_{\gamma_V}(\Theta\gamma_U + \Theta - 1) f_{\gamma_U}(\gamma_U)\,d\gamma_U,
\end{aligned}
\tag{9}
$$

where $\Theta = 2^{C_{th}}$. It should be noted that obtaining a closed-form result for Eq. (9) is almost impossible and/or too complex. Furthermore, it may be calculated by using numerical analysis [13]. To gain more insights, in the subsequent section, the lower bound of the DOP is proposed, which has been utilized in several others works such as [14], by

$$
P_{\text{DOP}}^{\text{L}} = \Pr\{\gamma_V \le \Theta\gamma_U\} = \int_0^\infty F_{\gamma_V}(\Theta x) f_{\gamma_U}(x)\,dx.
\tag{10}
$$

Lemma 3. $P_{\text{DOP}}^{\text{L}}$ is obtained as

$$
\begin{aligned}
P_{\text{DOP}}^{\text{L}} = 1 - \frac{6}{\alpha_V\alpha_U R_0}\cdot \\
\sum_{i=0}^{m-1}\frac{1}{i!}\sum_{j=1}^{2}\frac{\beta_j^3}{(-1)^j}G_{2,3}^{1,2}\left[\frac{\eta_2\Theta\rho_U}{\beta_j^{\alpha_U}}\,\Big|\,{1+\frac{3}{\alpha_U},1-\frac{2}{\alpha_V} \atop i,-\frac{2}{\alpha_V},\frac{3}{\alpha_U}}\right],
\end{aligned}
\tag{11}
$$

where $\beta_1 = r$ and $\beta_2 = R$. With the help of **Lemma 3**, the approximation of DOP, i.e. (9) can be obtained.

Proof: Substituting (3) and (6) into (10) and utilizing [11, (2.24.2.3)], one can obtain

$$
\begin{aligned}
P_{\text{DOP}}^{\text{L}} &= \int_0^\infty F_{\gamma_V}(\Theta x) f_{\gamma_U}(x)\,dx \\
&= 1 - \frac{2}{\alpha_V}\sum_{i=0}^{m-1}\frac{1}{i!}\int_0^\infty G_{1,2}^{1,1}\left[\eta_2\Theta x\,\Big|\,{1-\frac{2}{\alpha_V} \atop i,-\frac{2}{\alpha_V}}\right] f_{\gamma_U}(x)\,dx \\
&= 1 - \frac{6}{\alpha_V\alpha_U R_0}\sum_{i=0}^{m-1}\frac{1}{i!}\left(r^3 G_{2,3}^{1,2}\left[\frac{\eta_2\Theta\rho_U}{r^{\alpha_U}}\,\Big|\,{1+\frac{3}{\alpha_U},1-\frac{2}{\alpha_V} \atop i,-\frac{2}{\alpha_V},\frac{3}{\alpha_U}}\right]\right. \\
&\left. -R^3 G_{2,3}^{1,2}\left[\frac{\eta_2\Theta\rho_U}{R^{\alpha_U}}\,\Big|\,{1+\frac{3}{\alpha_U},1-\frac{2}{\alpha_V} \atop i,-\frac{2}{\alpha_V},\frac{3}{\alpha_U}}\right]\right) \\
&= 1 - \frac{6}{\alpha_V\alpha_U R_0}\sum_{i=0}^{m-1}\frac{1}{i!}\sum_{j=1}^{2}\frac{\beta_j^3}{(-1)^j}G_{2,3}^{1,2}\left[\frac{\eta_2\Theta\rho_U}{\beta_j^{\alpha_U}}\,\Big|\,{1+\frac{3}{\alpha_U},1-\frac{2}{\alpha_V} \atop i,-\frac{2}{\alpha_V},\frac{3}{\alpha_U}}\right],
\end{aligned}
\tag{12}
$$

where $\beta_1 = r$ and $\beta_2 = R$. ∎

In the simulation presented in Section V, one can see that the above expression matches the simulation results very well in most cases.

IV. AVERAGE DETECTION CAPACITY

In this paper, average detection capacity (ADC) is defined as the expected value of detection capacity of G2V over G2A, which can be given by

$$
\begin{aligned}
\bar{C}_s(\gamma_V,\gamma_U) &= E[C_s(\gamma_V,\gamma_U)] \\
&= \int_0^\infty\int_0^\infty C_s(\gamma_V,\gamma_U) f(\gamma_V,\gamma_U)\,d\gamma_V d\gamma_U,
\end{aligned}
\tag{13}
$$

where $f(\gamma_U,\gamma_V)$ is the joint PDF of γ_U and γ_V. The ADC is an important metric to estimate the average detection probability of home country's capacity to detect and/or eavesdrop the enemy's UAV.

As the detection and communication channels are independent with each other, we can rewrite ADC in (13) as

$$
\bar{C}_s = \underbrace{\frac{1}{\ln 2}\int_0^\infty\frac{\bar{F}_{\gamma_V}(x)}{1+x}\,dx}_{\triangleq\bar{C}_V} - \underbrace{\frac{1}{\ln 2}\int_0^\infty\frac{\bar{F}_{\gamma_V}(x)\bar{F}_{\gamma_U}(x)}{1+x}\,dx}_{\triangleq\bar{C}_{\text{Loss}}},
\tag{14}
$$

where $\bar{F}_{\gamma_U}(\gamma)$ and $\bar{F}_{\gamma_V}(\gamma)$ is the complementary CDF of γ_U and γ_V, and $\bar{C}_V$ denotes the ergodic capacity of the desired link, and $\bar{C}_{\text{Loss}}$ represents the capacity loss.

Lemma 4. $\bar{C}_V$ in (14) can be expressed as follows in closed form:

$$
\bar{C}_V = \frac{2}{\alpha_V\ln 2}\sum_{i=0}^{m-1}\frac{1}{i!}G_{2,3}^{2,2}\left[\eta_2\,\Big|\,{1-\frac{2}{\alpha_V},0 \atop i,0,-\frac{2}{\alpha_V}}\right].
\tag{15}
$$

Proof: By using **Lemma 2** and [12], $\bar{C}_V$ is as:

$$
\begin{aligned}
\bar{C}_V &= \frac{1}{\ln 2} \int_0^\infty \frac{\bar{F}_{\gamma_V}(x)}{1+x} dx \\
&= \frac{2}{\alpha_V \ln 2} \sum_{i=0}^{m-1} \frac{1}{i!} \int_0^\infty \frac{1}{1+x} G_{1,2}^{1,1}\left[\eta_2 x \left| \begin{matrix} 1-\frac{2}{\alpha_V} \\ i, -\frac{2}{\alpha_V} \end{matrix} \right. \right] dx \\
&= \frac{2}{\alpha_V \ln 2} \sum_{i=0}^{m-1} \frac{1}{i!} \int_0^\infty G_{1,1}^{1,1}\left[x \left| \begin{matrix} 0 \\ 0 \end{matrix} \right. \right] G_{1,2}^{1,1}\left[\eta_2 x \left| \begin{matrix} 1-\frac{2}{\alpha_V} \\ i, -\frac{2}{\alpha_V} \end{matrix} \right. \right] dx \\
&= \frac{2}{\alpha_V \ln 2} \sum_{i=0}^{m-1} \frac{1}{i!} G_{2,3}^{2,2}\left[\eta_2 \left| \begin{matrix} 1-\frac{2}{\alpha_V}, 0 \\ i, 0, -\frac{2}{\alpha_V} \end{matrix} \right. \right].
\end{aligned}
\tag{16}
$$

Then, the proof is completed. ∎

By using **Lemma 1** and **Lemma 2**, one can have $\bar{C}_{\text{Loss}}$ as

$$
\begin{aligned}
\bar{C}_{\text{Loss}} &= \frac{2}{\alpha_V \ln 2} \sum_{i=0}^{m-1} \frac{1}{i!} \int_{\frac{\rho_U}{R^{\alpha_U}}}^{\frac{\rho_U}{r^{\alpha_U}}} \frac{1}{1+x} G_{1,2}^{1,1}\left[\eta_2 x \left| \begin{matrix} 1-\frac{2}{\alpha_V} \\ i, -\frac{2}{\alpha_V} \end{matrix} \right. \right] \cdot \\
&\left(\frac{(\rho_U)^{\frac{3}{\alpha_U}}}{R_0} x^{-\frac{3}{\alpha_U}} - \frac{r^3}{R_0} \right) dx + \frac{2}{\alpha_V \ln 2} \cdot \\
&\sum_{i=0}^{m-1} \frac{1}{i!} \int_0^{\frac{\rho_U}{R^{\alpha_U}}} \frac{1}{1+x} G_{1,2}^{1,1}\left[\eta_2 x \left| \begin{matrix} 1-\frac{2}{\alpha_V} \\ i, -\frac{2}{\alpha_V} \end{matrix} \right. \right] dx.
\end{aligned}
\tag{17}
$$

Similar to [7], one can apply Gaussian-Chebyshev quadrature to get the closed-form solution of (17) by using [15, Eq. (25.4.30)] or calculate it numerically, which is omitted here to make the paper compact. Then, $\bar{C}_s$ can be computed by using $\bar{C}_V$ in (16) and $\bar{C}_{\text{Loss}}$ in (17). In the next section, we will show the numerical results.

V. NUMERICAL RESULTS AND DISCUSSIONS

In this section, Monte Carlo simulations are conducted to validate the effectiveness of the derived DOP and ADC. The simulations are conducted by using Matlab 2018a and the curves labelled 'Simulation' are obtained by randomly and uniformly deploying the UAV in the specified region for 10^6 times. For Figs. 2 - 4, we evaluate the performance of the DOP, where the 'Approximation' curve is obtained by **Lemma 3**. For Figs. 5 - 7, we examine the performance of the ADC, where the 'Approximation' curve is obtained by **Lemma 4** and (17).

A. DOP

For Figs. 2 - 4, we show the DOP versus D for various r, where $C_{th} = 1$ bit/s/Hz is set in these figures. In Fig. 2, we assume $m = 1$, $R = 12000$ m, $\alpha_V = 2$, $\alpha_U = 2$, $\rho_U = \rho_V = 130$ dB, where one can see that with the increase of detection distance D, the DOP increases. This is because with the increase of the distance from the GV to GS, the SNR of G2V link decreases, and therefore the detection capacity deteriorates. Also, one sees that with the increase of communication distance of UAV r, the DOP decreases. This is because it is easier to detect UAV when UAV flies far from the GS, as GS may increase the SNR to communicate with UAV, resulting in better SNR received by GV for detection.

In Fig. 3, we increase m from 1 to 2 while keeping the other parameters unchanged. Comparing Fig. 3 with Fig. 2, one sees
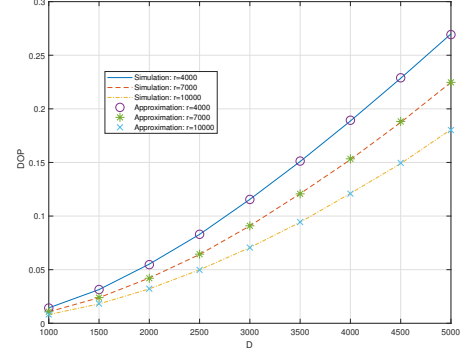

Fig. 2. DOP versus D for $r = 4000$ m, 7000 m and 10000 m, with $m = 1$, $R = 12000$ m, $\alpha_V = 2$, $\alpha_U = 2$ and $\rho_U = \rho_V = 130$ dB.
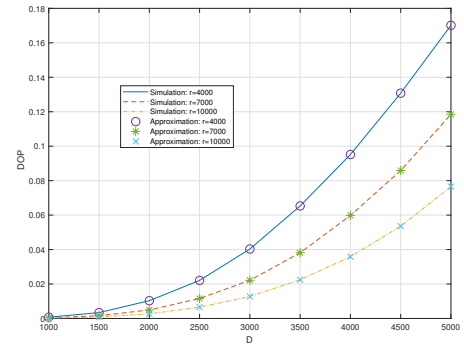

Fig. 3. DOP versus D for $r = 4000$ m, 7000 m and 10000 m, with $m = 2$, $R = 12000$ m, $\alpha_V = 2$, $\alpha_U = 2$ and $\rho_U = \rho_V = 130$ dB.

that the DOP decreases. This is because when m changes from 1 to 2, the fading is less serious in the environment, and thus resulting in lower DOP. In Fig. 4, we examine the DOP versus D with the path loss parameter setting to $\alpha_V = 4$ and $\alpha_U = 4$. We also increase $\rho_U = \rho_V = 220$ dB to combat the severe path loss. This figure shows the scenario that both the UAV and GV experience the serious path loss. Similarly, one can see that in Fig. 4, with the increase of detection distance in G2V link or decrease of communication distance in G2A link, the DOP
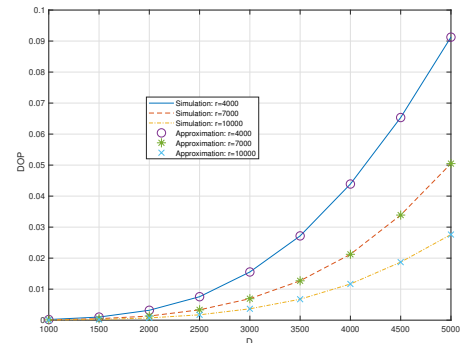

Fig. 4. DOP versus D for $r = 4000$ m, 7000 m and 10000 m, with $m = 1$, $R = 12000$ m, $\alpha_V = 4$, $\alpha_U = 4$ and $\rho_U = \rho_V = 220$ dB.

increases, as the reason explained before. Additionally, one can see that with the increase of the communication distance r or the decrease of detection distance D, the DOP reduces, resulting in better detection performance.

In all these cases above, one can see that our approximation of DOP matches well with the simulation results, showing the accuracy and the usefulness of our proposed expression.

B. ADC

In this subsection, we check the performance of ADC. In Figs. 5 - Fig. 7, we examine the ADC versus D for various r, where $C_{th} = 1$ bit/s/Hz is set in these figures. In Fig. 5, we set $m = 1$, $R = 12000$ m, $\alpha_V = 2$, $\alpha_U = 2$ and $\rho_U = \rho_V = 130$ dB. One can see that with the increase of
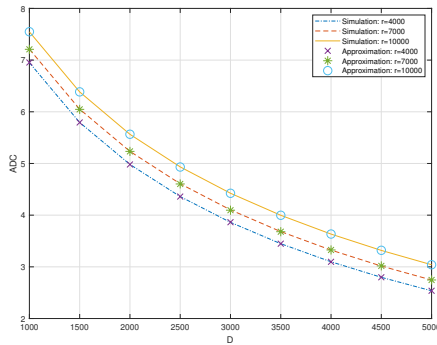

Fig. 5. ADC versus D for $r = 4000$ m, 7000 m and 10000 m, with $m = 1$, $R = 12000$ m, $\alpha_V = 2$, $\alpha_U = 2$, $\alpha_U = 2$ and $\rho_U = \rho_V = 130$ dB.

the detection distance, the ADC decreases. This is because the farther the GV is, the less received SNR the G2V link achieves, and therefore resulting in lower ADC. Moreover, one can see that with the increase of the communication distance of UAV r, the ADC increases. This is because with the increase of r, the SNR gap between the G2V link and G2A link increases, resulting in better ADC.

From Fig. 6 to Fig. 5, we increase the Nakagami fading parameter m from 1 to 2. One can see that the ADC increases. This is because the less serious fading will improve the detection capacity. In Fig. 7, we examine the ADC versus D
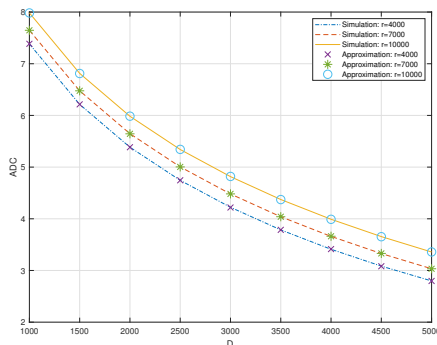

Fig. 6. ADC versus D for $r = 4000$ m, 7000 m and 10000 m, with $m = 2$, $R = 12000$ m, $\alpha_V = 2$, $\alpha_U = 2$ and $\rho_U = \rho_V = 130$ dB

for various r with the path loss exponent setting to $\alpha_V = 4$, $\alpha_U = 4$, which shows both UAV and GV experience serious path loss. Similarly with before, one can see that with the increase of the detection distance D, or decrease of communication distance r, the ADC decreases, as expected.
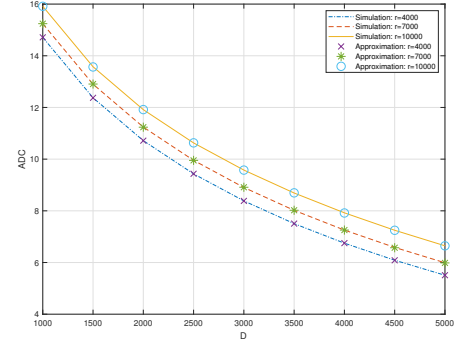

Fig. 7. ADC versus D for $r = 4000$ m, 7000 m and 10000 m, with $m = 1$, $R = 12000$ m, $\alpha_V = 4$, $\alpha_U = 4$ and $\rho_U = \rho_V = 220$ dB

Again, in all these tests above, one can see that our 'Approximation' curve match well with the simulation results, showing the effectiveness and usefulness of our derived expressions.

VI. CONCLUSION

In this paper, we have investigated the DOP and ADC of G2V over G2A communication systems. Exact expressions have been shown and to get more insights, tight analytical approximations have been obtained. One sees that with the decrease of detection distance or the increase of the communication region or the decrease of the fading influence, the DOP drops while the ADC improves. Numerical results have been carried out to verify the effectiveness of the derived expressions. Future work will focus on multi-UAV scenarios, such as how to detect multiple UAVs applying the ground vehicles or deploy the UAVs from home country to detect the enemy's UAVs. Also, multiple antennas in both UAVs and ground stations will be explored. Furthermore, the impact of interference will be taken into consideration in future work.

REFERENCES

[1] Alzahrani, Bander, Omar Sami Oubbati, Ahmed Barnawi, Mohammed Atiquzzaman, and Daniyal Alghazzawi, "UAV assistance paradigm: State-of-the-art in applications and challenges," *Journal of Network and Computer Applications*, pp. 102706, 2020.

[2] O. S. Oubbati, N. Chaib, A. Lakas, P. Lorenz and A. Rachedi, "UAV-Assisted Supporting Services Connectivity in Urban VANETs," in IEEE Transactions on Vehicular Technology, vol. 68, no. 4, pp. 3944-3951, April 2019.

[3] M. Zenko, *Reforming US drone strike policies*. Council on Foreign Relations, no. 65,2013.

[4] D. H. Lyon, "A military perspective on small unmanned aerial vehicles," *IEEE Instrum. Meas. Mag.*, vol. 7, no. 3, pp. 27-31, Sept. 2004.

[5] G. Chen, Y. Gong, P. Xiao and J. A. Chambers, "Physical Layer Network Security in the Full-Duplex Relay System," *IEEE Transactions on Information Forensics and Security*, vol. 10, no. 3, pp. 574-583, March 2015.

[6] J. Ye, C. Zhang, H. Lei, G. Pan and Z. Ding, "Secure UAV-to-UAV Systems With Spatially Random UAVs," *IEEE Wireless Commun. Lett.*, vol. 8, no. 2, pp. 564-567, April 2019.

[7] H. Ren, C. Pan, K. Wang, Y. Deng, M. Elkashlan and A. Nallanathan, "Achievable Data Rate for URLLC-Enabled UAV Systems With 3-D Channel Model," *IEEE Wireless Commun. Lett.*, vol. 8, no. 6, pp. 1587-1590, Dec. 2019.

[8] K. Wang, C. Pan, H. Ren, W. Xu, L. Zhang and A. Nallanathan, "Packet Error Probability and Effective Throughput for Ultra-reliable and Low-latency UAV Communications," *IEEE Transactions on Communications*, 2020

[9] H. Lei, C. Gao, I. S. Ansari, Y. Guo, Y. Zou, G. Pan, and K. Qaraqe, "Secrecy outage performance of transmit antenna selection for MIMO underlay cognitive radio systems over Nakagami-m channels," *IEEE Trans. Veh. Technol.*, vol. 66, no. 3, pp. 2237-2250, Mar. 2017.

[10] I. S. Gradshteyn and I. M. Ryzhik, *Table of Integrals, Series and Products*, 7th. San Diego,CA: Academic Press, 2007.

[11] A. P. Prudnikov, Y. A. Brychkov, and O. I. Marichev, *Integrals and Series: Vol. 3: More Special Functions*. New York: CRC Press, 1992.

[12] V. S. Adamchik and O. I. Marichev, "The algorithm for calculating integrals of hypergeometric type functions and its realization in REDUCE system," in *Proc. the international symposium on Symbolic and algebraic computation (ISSAC'90)*, Tokyo, Japan, Aug. 1990, pp. 212-224.

[13] E. Hildebrand, *Introduction to numerical analysis*. NewYork, NY, USA, Dover, 1987.

[14] H. Lei, H. Luo, K.-H. Park, G. Pan, Z. Ren, and M.-S. Alouini, "Secrecy outage analysis of mixed RF-FSO systems with channel imperfection," *IEEE Photon. J.*, vol. 10, no. 3, pp. 1-14, Jun. 2018.

[15] M. Abramowitz and I. A. Stegun, *Handbook of Mathematical Functions with Formulas, Graphs, and Mathematical Tables, 9th ed.* Handbook of Mathematical Functions with Formulas, Graphs, and Mathematical Tables, 1972.